REPORT DOCUMENTATION PAGE

Form Approved
OMB NO. 0704-0188

1. AGENCY USE ONLY (Leave Blank)	2. REPORT DATE	3. REPORT TYPE AND DATES COVERED
	November 4, 2004	Final Report , August 7, 2003 – August 6, 2004

4. TITLE AND SUBTITLE

Support for Advanced Imaging of Premixed Turbulent Combustion Processes

5. FUNDING NUMBERS

DAAD19-03-1-0251

6. AUTHOR(S)

F. C. Gouldin

7. PERFORMING ORGANIZATION NAME(S) AND ADDRESS(ES)

Cornell University, Ithaca, NY 14853

8. PERFORMING ORGANIZATION REPORT NUMBER

9. SPONSORING / MONITORING AGENCY NAME(S) AND ADDRESS(ES)

U. S. Army Research Office
P.O. Box 12211
Research Triangle Park, NC 27709-2211

10. SPONSORING / MONITORING AGENCY REPORT NUMBER

45741.1-EG

11. SUPPLEMENTARY NOTES

The views, opinions and/or findings contained in this report are those of the author(s) and should not be construed as an official Department of the Army position, policy or decision, unless so designated by other documentation.

12 a. DISTRIBUTION / AVAILABILITY STATEMENT

Approved for public release; distribution unlimited.

12 b. DISTRIBUTION CODE

13. ABSTRACT (Maximum 200 words)

The laser imaging diagnostics of crossed-plane laser tomography (CPLT) and stereo particle image velocimetry (SPIV) have been combined for a systematic study of premixed turbulent combustion in CH_4-air, V- burner and swirl-burner flames. Data sets comprised of between 1500 and 2000 realizations have been obtained for 11 different V-flame conditions and 5 different swirl-burner flame conditions.

These raw data sets are being analyzed to build a unique database that quantifies mean flame properties (e.g., mean progress variable fields), chemical reaction sheet wrinkling by turbulence (e. g., reaction sheet orientation statistics, curvatures and surface density data) and important velocities (e. g., velocity field of reactants, reaction sheet displacement speeds and gas velocity correlations at the reaction sheet surface). The most significant finding to date is that of negative displacement speeds and a correlation between displacement speed and reaction sheet curvature. These developments are outlined in this report.

14. SUBJECT TERMS

premixed turbulent combustion, laser tomography, velocimetry, flamelet displacement speed, curvature

15. NUMBER OF PAGES

16 17

16. PRICE CODE

17. SECURITY CLASSIFICATION OR REPORT	18. SECURITY CLASSIFICATION ON THIS PAGE	19. SECURITY CLASSIFICATION OF ABSTRACT	20. LIMITATION OF ABSTRACT
UNCLASSIFIED	**UNCLASSIFIED**	**UNCLASSIFIED**	**UL**

NSN 7540-01-280-5500

Standard Form 298 (Rev.2-89)
Prescribed by ANSI Std. 239-18
298-102

Final Report for DAAD19-03-1-0251
Support for Advanced Imaging of Premixed Turbulent Combustion Processes

Table of Contents

Form 298 Continuation sheets
Final Report for DAAD19-03-1-0251
Support for Advanced Imaging of Premixed Turbulent Combustion Processes

1) Statement of Problem Studied

For a broad range of turbulent flow conditions the effect of flow turbulence on premixed flames is to wrinkle and distort the flame sheet thereby increasing combustion rates per unit volume – the combustion intensity. In previous ARO sponsored research we developed crossed-plane imaging methods for the study of reaction sheet wrinkling (crossed-plane laser tomography) and changes in reaction sheet thermal structure (crossed-plane Rayleigh imaging) due to turbulence. In the present research we combine crossed-plane laser tomography (CPLT) with stereo particle image velocimetry (SPIV) to measure flamelet wrinkling, flamelet speeds and the reactant velocity field in order to relate flamelet properties to the turbulent velocity field in the reactant flow.

And Summary of Important Results

Using combined CPLT and SPIV we have obtained a large data set for 11 different flames stabilized in a V-flame burner and 5 different flames stabilized in a swirl-flame burner. We are in the process of analyzing these data and have concentrated so far on the V-flame burner data. The most significant finding to date is the presence of negative displacement speeds and a correlation between displacement speed and flamelet curvature. Negative displacement speeds have be predicted but this is the first time they have been observed in turbulent flames. Details of the measurements and results to date are given below.

2) List of Publications / Papers

(a) D. A. Knaus, S. S. Sattler and F. C. Gouldin, Crossed-plane Rayleigh Imaging for Three - Dimensional Temperature Gradients in Premixed Turbulent Flamelets, submitted March 2004 to *Combustion and Flame*, accepted November 2004. Research supported under DAAD19-99-0324 and DAAD19-03-1-0251.

(b) Combined Crossed-Plane Tomography and Stereo Particle Image Velocimetry – Flamelet Displacement Speeds", S. S. Sattler and F. C. Gouldin, submitted December 2003 to the 30th Combustion Symposium. Not accepted; under revision for submission to *Combustion and Flame*.

(c) Determination of Flamelet Curvature from Crossed-Plane Image Data, F. C. Gouldin and S. S. Sattler, AIAA 2004-0976, presented at the 42nd Aerospace Sciences Meeting, January 2004, Reno, NV.

(d) Downstream Development of Premixed Turbulent V-Flames, R. Beresky, S. S. Sattler and F. C. Gouldin, AIAA 2005-0153, to be presented at the 43nd Aerospace Sciences Meeting, January 2005, Reno, NV.

(c) Support for Advanced Imaging of Premixed Turbulent Combustion Processes, Interim report to ARO, F. C. Gouldin, April 30, 2003

Paper demographic data for Life of Grant

4 papers submitted and 1 paper presented.

3) List of Participants

The following students worked on grant related research but were not financially supported:

Sandra Sattler	PhD student, expected to graduate in June 2005
Soo Ho Lee	MEng student, graduated in May 2004
Ian Bell	BS student, expected to graduate in May 2006
Ryan Beresky	BS student, expected to graduate in January 2005
Joonil Kwak	BS student, graduated in May 2004

4) Inventions: none

5) Technology transfer: none.

6) Scientific Progress and Accomplishments

ADVANCED IMAGING OF PREMIXED TURBULENT COMBUSTION PROCESSES

F. C. Gouldin
Mechanical and Aerospace Engineering
Cornell University, Ithaca, NY 14853

Introduction

Over the last several years at Cornell we have developed and applied advanced imaging methods – crossed-plane laser tomography (CPLT) [1 – 5], crossed-plane laser Rayleigh imaging [6] and stereo particle image velocimetry (SPIV) -- for high-resolution studies of scalar and velocity fields in premixed turbulent combustion. Pulsed laser tomography with micron sized, silicone oil droplets can be used to image the intersections of 650 K isothermal surfaces and the laser illumination plane. We have used CPLT to measure the instantaneous orientation of these surfaces and to determine the probability density function of the surface normal vector, a statistical measure of surface wrinkling that is used to calculate the mean surface to volume ratio or the surface density of the 650 K surface. More recently, we have combined CPLT and SPIV [7] in order to simultaneously measure the surface normal, the reactant velocity field and the reaction sheet (flamelet) displacement speed in the laboratory reference frame and relative to the local reactant gas velocity. In addition numerical experiments have been used to evaluate the potential for using CPLT to measure the principle curvatures of the wrinkled reaction sheet in addition to the sheet normal vector.

The goal of our current research is to exploit combined CPLT and SPIV in a systematic study of premixed turbulent combustion in a V-flame burner and a swirl burner. The expected result of this study will be a unique database that quantifies both reaction sheet wrinkling by turbulence (reaction sheet normal vectors, principle curvatures and surface density data) and velocities (velocity field of reactants, displacement speeds and velocity correlations at the reaction sheet surface).

To this end we have made measurements of flamelet displacement speed in a methane – air V-flame, looked at measurements of curvature in V-flames, built a swirl burner based on a design by Robert Cheng at Lawrence Berkeley National Laboratory, and taken combined CPLT and SPIV data on a total of eleven turbulent, premixed methane-air, V-flames and on five swirl burner flames. These developments are outlined in this report.

The people working on the research covered by this report are the PI, Sandra Sattler, a Ph.D. student, Soo Ho Lee, a M. Eng. student and three undergraduate students – Ian Bell, Ryan Beresky and Joonil Kwak. Research into curvature determination was reported at the last AIAA Aerospace Sciences Meeting. In addition a manuscript reporting on previous work support by ARO was submitted to *Combustion and Flame* [6] and has been accepted.

Method and Quantities Measured

Combined Crossed-Plane Laser Tomography and Stereo Particle Imaging Velocimetry: SPIV allows one to measure a 2-D distribution of the 3-D velocity vector field. For SPIV, two CCD cameras, mounted in a Scheimpflug configuration, are focused from different angles onto the same plane. Each camera takes two exposures of laser light scattering from seed particles in the flow at two closely spaced points in time. The measured displacements of the seed particles between exposures are used to determine particle and thereby gas velocities. A single camera can be used to obtain the in-plane velocity components; images from a pair of cameras allow one to estimate the out-of-plane velocity component as well as the in-plane components. A double-pulsed, dual-head, frequency doubled, 130 mJ/pulse Nd:YAG laser fired sequentially in time is the light source for these measurements. The beams from the two laser heads are aligned collinearly and formed into overlapping sheets in the image plane of the cameras. The laser and image acquisition cameras are controlled by a data acquisition and analysis computer. A commercial SPIV system including laser, optics, cameras and computer is used for the measurements. The camera and laser sheet configuration used for combined SPIV and CPLT is shown in Fig. 1.

In CPLT, images of seed particle scattering are taken near simultaneously from two intersecting, orthogonal laser sheets. The seed particles are micron sized silicone oil drops that evaporate on or near the 650 K isothermal surface [8]. In each image a curve marking the disappearance of the droplets and therefore the 650 K isotherm is identified. Tangent vectors to these curves projected onto the illumination planes are tangent vectors to the 650 K surface. Where this surface crosses the line of intersection between the two illumination planes, two tangent vectors can be determined and their cross product is normal to the 650 K surface at the instant the images are taken. Repeated laser firing and image pair acquisition makes it possible to generate PDF's of surface normal vectors.

Using oil seed with combined SPIV and CPLT one can obtain the distribution of reactant velocities in a vertical plane and the 650 K surface normal vectors over a 100 microsecond time period. These velocities and surface normal vectors are found at the three points where the 650 K surface crosses the three horizontal lines of intersection between the laser illumination planes. These lines are marked a, b and c in Fig. 2. In addition, by staggering the pulse-timings of the tomography laser and the SPIV lasers by approximately 1.5 milliseconds, displacement speeds of the 650 K surface in the laboratory frame and relative to the gas flow are determined.

The data obtained from combined CPLT - SPIV measurements can be used in several different ways. Normal vector data can be used to find the 650 K sheet surface density, an important modeling term that is proportional to the mean rate of product formation. The PDF of the sheet normal vector is one measure of the wrinkling of the sheet by the turbulence as is the PDF of the principle radii of curvature. Reaction sheet structure is perturbed by the turbulent flow field through imposed flow strain and curvature. The reactant field velocity data obtained with SPIV and CPLT can be used to estimate elements of imposed strain. Also of importance is the displacement speed on the cold side of the reaction sheet, which is the difference between the component of the gas velocity on the reactant side normal to the reaction sheet and the sheet speed in the laboratory frame.

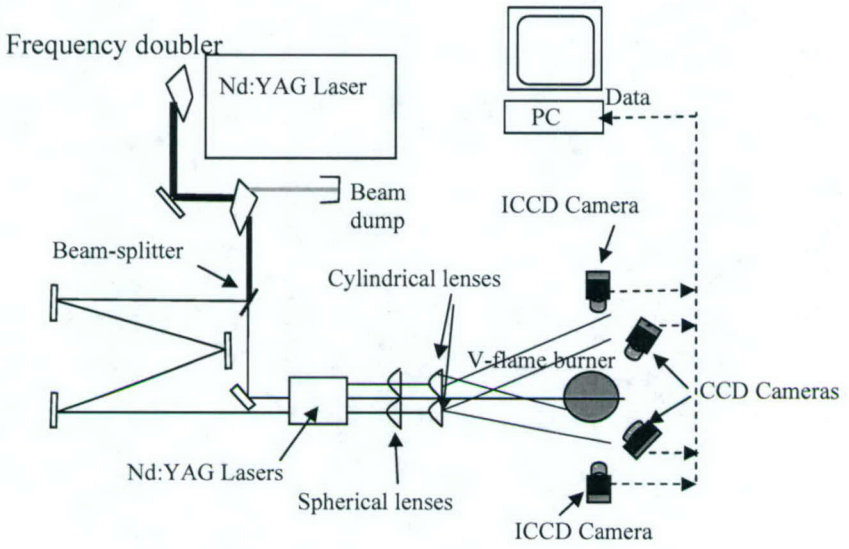

Figure 1. Schematic diagram of combined SPIV and CPLT system showing the overall layout of the system including lasers, cameras, optics and burner. The laser sheets propagate out of the plane of the paper. To avoid over-exposing the cameras to laser pulses, the CPLT images are taken first. The SPIV images are taken approximately 1.5 milliseconds later. Surface normal vectors are measured where the 650 K surface crosses the three lines of intersection, denoted by a, b, and c in figure 2, between the three illumination planes defined by laser sheets 1 and 2 and the SPIV laser sheet. Velocity vectors are obtained over the vertical SPIV laser sheet. The field of view of each of the four cameras is approximately 35mm x 35mm. The tomography cameras have 512 x 512 pixels, while the PIV cameras have 1360 x 1030 pixels.

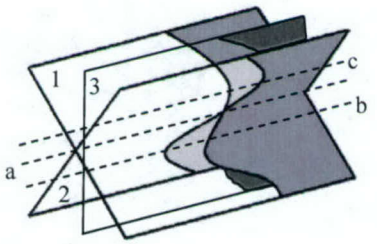

Figure 2. Schematic of combined CPLT-SPIV laser-sheet orientations. 1 and 2 are the perpendicular CPLT laser sheets and lie at 45^0 with respect to 3, the vertical SPIV laser sheet. The sheets intersect forming three measurement lines: a, b, and c. Flamelet normals and displacement speeds are measured along lines b and c; flamelet normals are measured along a.

Results to Date

Data Taken: Data sets consisting of CPLT and SPIV images have been collected for 11 different V-flames. The flame parameters are listed in Table 1, and the location of each flame on the Peters regime diagram [9] is shown in Figure 3. Each data realization consists of two tomography images and four SPIV images; for each flame condition images from approximately 2000 realizations have been obtained for data analysis. Similar data sets have been obtained for 5 swirl burner flames, see Table 3. Our current focus of analysis using these image sets is the determination of displacement speed and flamelet curvature and characterization of the reactant flow turbulence.

Table 1. V-Flames Conditions

Flame #	l/l_f	u'/S_L^0	U_0(m/s)	ϕ	M(mm)
1	33.6	0.6	2	0.65	4.2
2	48	1.5	2	0.65	6
3	33.6	1.17	4	0.65	4.2
4	48	2.68	4	0.65	6
5	58.8	0.628	4	0.8	4.2
6	84	1.44	4	0.8	6
7	44.1	0.57	2.61	0.7	4.2
8	44.1	1.023	4.21	0.7	4.2
9	42	1	6	0.7	4.2
10	31.5	3.16	5.3	0.7	perforated plate
11	48	1.85	3	0.65	6

The length scale ratio, l/l_f, is the ratio of the turbulence integral scale to the flame thickness; u'/S_L^0 is the turbulence intensity divided by the unstretched laminar flame speed; U_0(m/s) is the mean flow speed upstream of the flame stabilizing rod; ϕ is the equivalence ratio; and finally, M(mm) is the mesh spacing of the turbulence generating grid; the fuel is methane.

Flamelet Displacement Speed Measurements: For steady, unstretched premixed laminar flames, the mass flux across an isothermal surface is independent of the surface and when divided by the reactant gas density at the surface yields the unstretched laminar burning velocity, S_L^0. In a turbulent flame, the flow is unsteady; the flamelet is curved; and the local mass flux across isothermal surfaces varies in space and time. These variations are one measure of flamelet distortion by turbulence. A related measure is the flamelet displacement speed, S_d, that we define here as the component of the instantaneous gas velocity relative to the flamelet and perpendicular to the instantaneous flamelet surface, as determined by crossed-plane tomography, the 650 K surface.

In combined CPLT and SPIV, $\underline{N}$ is measured along three parallel measurement lines (see Figure 3) and $\underline{U}_r(x,y)$ is measured in a vertical plane. Along the measurement lines in the SPIV plane, $\underline{N}$, $\underline{U}_r$ and displacement speeds are obtained. To determine displacement speed, data on flamelet position, as marked by the 650 K isotherm, on the two measurement lines in the SPIV plane are obtained in each of the camera images. The laser pulse timings of these images are staggered and the flamelet displacement speed along a measurement line in the laboratory reference frame is obtained by analyzing the

Results to Date

Data Taken: Data sets consisting of CPLT and SPIV images have been collected for 11 different V-flames. The flame parameters are listed in Table 1, and the location of each flame on the Peters regime diagram [9] is shown in Figure 3. Each data realization consists of two tomography images and four SPIV images; for each flame condition images from approximately 2000 realizations have been obtained for data analysis. Similar data sets have been obtained for 5 swirl burner flames, see Table 3. Our current focus of analysis using these image sets is the determination of displacement speed and flamelet curvature and characterization of the reactant flow turbulence.

Table 1. V-Flames Conditions

Flame #	l/l_f	u'/S_L^0	U_0(m/s)	ϕ	M(mm)
1	33.6	0.6	2	0.65	4.2
2	48	1.5	2	0.65	6
3	33.6	1.17	4	0.65	4.2
4	48	2.68	4	0.65	6
5	58.8	0.628	4	0.8	4.2
6	84	1.44	4	0.8	6
7	44.1	0.57	2.61	0.7	4.2
8	44.1	1.023	4.21	0.7	4.2
9	42	1	6	0.7	4.2
10	31.5	3.16	5.3	0.7	perforated plate
11	48	1.85	3	0.65	6

The length scale ratio, l/l_f, is the ratio of the turbulence integral scale to the flame thickness; u'/S_L^0 is the turbulence intensity divided by the unstretched laminar flame speed; U_0(m/s) is the mean flow speed upstream of the flame stabilizing rod; ϕ is the equivalence ratio; and finally, M(mm) is the mesh spacing of the turbulence generating grid; the fuel is methane.

Flamelet Displacement Speed Measurements: For steady, unstretched premixed laminar flames, the mass flux across an isothermal surface is independent of the surface and when divided by the reactant gas density at the surface yields the unstretched laminar burning velocity, S_L^0. In a turbulent flame, the flow is unsteady; the flamelet is curved; and the local mass flux across isothermal surfaces varies in space and time. These variations are one measure of flamelet distortion by turbulence. A related measure is the flamelet displacement speed, S_d, that we define here as the component of the instantaneous gas velocity relative to the flamelet and perpendicular to the instantaneous flamelet surface, as determined by crossed-plane tomography, the 650 K surface.

In combined CPLT and SPIV, $\underline{N}$ is measured along three parallel measurement lines (see Figure 3) and $\underline{U}_r(x,y)$ is measured in a vertical plane. Along the measurement lines in the SPIV plane, $\underline{N}$, $\underline{U}_r$ and displacement speeds are obtained. To determine displacement speed, data on flamelet position, as marked by the 650 K isotherm, on the two measurement lines in the SPIV plane are obtained in each of the camera images. The laser pulse timings of these images are staggered and the flamelet displacement speed along a measurement line in the laboratory reference frame is obtained by analyzing the

stored images to determine the flamelet travel distance between the laser pulses. In turn this speed is used along with $\underline{U_r}$ and $\underline{N}$ data to estimate the normalized flamelet displacement speed relative to reactants, S_d/S_L^o.

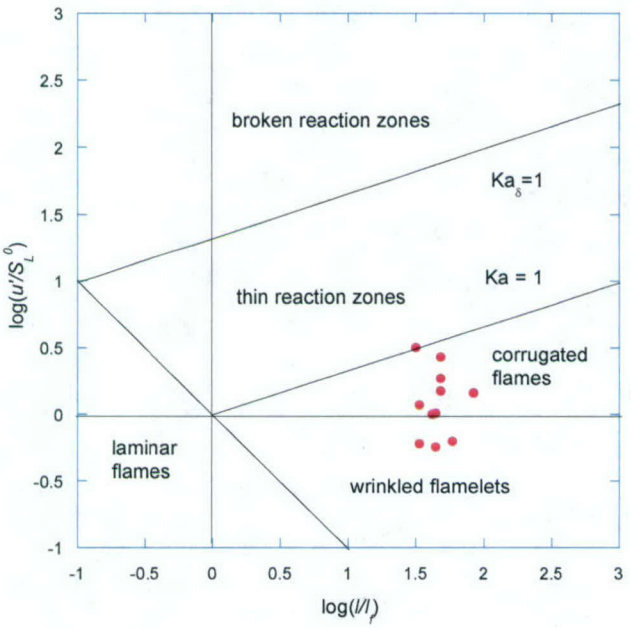

Figure 3. Peters regime diagram showing conditions of the 11 flames studies. Ka is the Karlovitz number based on l_f, the flame thickness; Ka_δ the Karlovitz number based on the high temperature reaction zone thickness, δ.

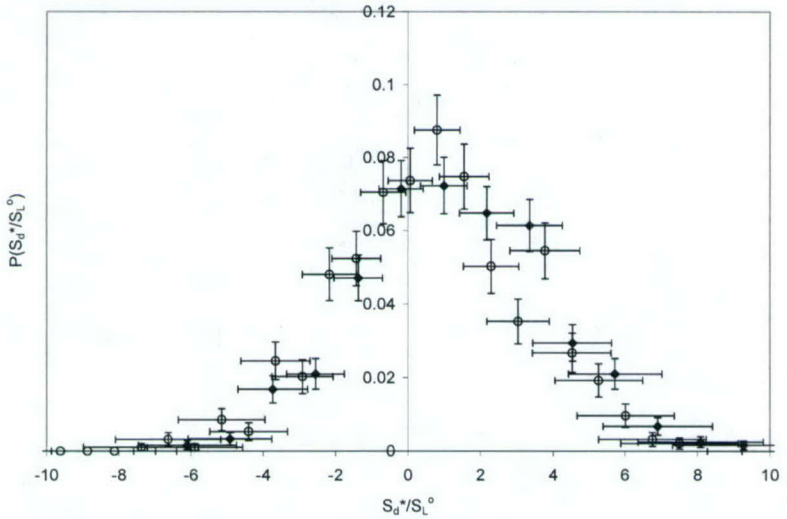

Figure 4a. Measured, density weighted, flamelet displacement speed relative to reactants. Data from the two measurement lines in the PIV plane are shown.

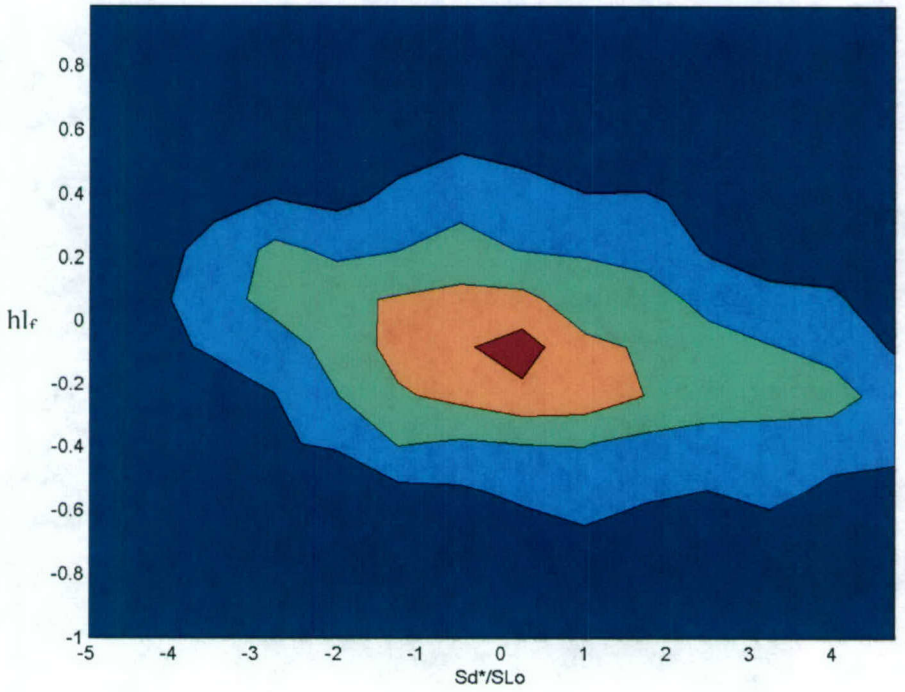

Figure 4b. Joint pdf of curvature, h, scaled by the laminar flame thickness and density weighted displacement speed scaled by the unstrained laminar flame speed.

The technique has been used so far to measure S_d^*/S_L^o in a lean, premixed, methane-air turbulent V-flame, flame 1 in Table 1. The displacement speed measured is that of approximately the 650 K isothermal surface. To account for acceleration within the flamelet, the speed is reported as S_d^*, the density weighted displacement speed, the product of the measured displacement speed and the density at 650 K divided by the reactant density. Flamelet normal data were also obtained. These latter data are consistent with data taken in previous 90° CPLT studies of V and spark-ignition engine flames [1 - 3]. The measured probability density function of the flamelet normal is fit by a universal form characterized by a single fit parameter, ζ. ζ is the same on the three measurement lines, within experimental uncertainty.

The displacement speed results for this flame are shown in Figure 4 where it can be seen that the distribution of S_d^*/S_L^o is peaked with a mean of approximately 1.7±1 and broad ($-5<S_d/S_L^o<7$). The vertical error bars in the figure indicate statistical uncertainty and are proportional to $1/(n)^{1/2}$, where n is the number of samples in each histogram bin used to construct the distribution. The horizontal error bars are estimated by the rms error given in [4, 10] and the uncertainty analysis detailed in [11]. The experimental uncertainty estimates of the SPIV data are based on test results reported in [10]. Negative displacement speeds are not entirely unexpected. For example, they have been predicted

to occur in highly strained opposed jet flames [12] and observed experimentally in double flames stabilized on an opposed jet burner [13]. In addition they have been seen in a DNS of the interaction of a flame with a counter-rotating vortex pair [14] and in a 2-D DNS of a turbulent methane-air flame [15]. The negative displacement speeds observed in the latter calculation are attributed to regions of high positive curvature and extensive tangential strain. From our 2-D image data we have estimated curvature in the plane of the laser illumination sheet and investigated the correlation between S_d^* and 2-D curvature. Figure 4b shows the joint PDF of S_d^*/S_L^0 and 2-D curvature scaled by the unstrained laminar flame speed. These data show that the two are correlated and that negative curvature is likely to increase S_d^* and the opposite for positive curvature.

Downstream development of premixed turbulent V-flames: In a previous study [5] it was found that measures of flamelet wrinkling and mean turbulent combustion rate increase linearly with downstream distance from the flame holder. A goal of the present research has been to use CPLT-SPIV data to explain variations in the rates of increase observed from flame condition to flame condition. For example data for the variation of the PDF fit parameter versus distance are shown in Figure 5. In our work on this problem we are currently using CPLT-SPIV data to calculate quantities charactering the reactant flow turbulence and its downstream development, e.g., turbulent intensity, turbulent integral and Taylor scales and components of the reactant velocities parallel and perpendicular to the flamelet. Our goal is to see if variations in these quantities can explain variations in flamelet wrinkling and combustion rate growth between flames.

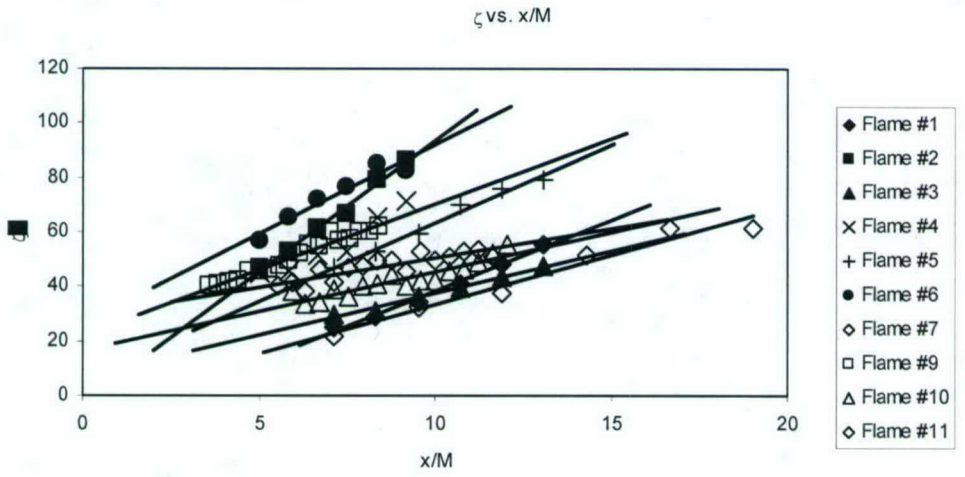

Figure 5. Downstream development of fit parameters for the eleven flames studied and straight line fits of data.

3-D Curvature determination: The principle curvatures of a surface provide a local description of that surface as the altitude of the surface above a tangent plane of the surface. If x_t and y_t form a right-handed coordinate system in the tangent plane with its

origin at the point of tangency between the plane and the surface, the surface altitude above the tangent plane in the vicinity of the origin is given by

$$h_s(x,y) = c_x x_t^2 + c_y y_t^2 \qquad (1)$$

c_x and c_y are the principle curvatures of the surface [16, 17], and the quantities that we wish to measure. Small values of these coefficients mean large radii of curvature.

In CPLT the two laser illumination planes are aligned orthogonal to each other, and their line of intersection, the measurement line, is horizontal. The tomography images can be processed to obtain the flamelet curves in each image that are the intersection of the 650 K isotherm of the flamelet and the laser illumination plane. From third order polynomial fits of these curves, flamelet curve tangent vectors are obtained in each illumination plane at the points where the flamelet curves intersect the measurement line. The cross product of these two tangent vectors gives the flamelet normal vector and defines the flamelet tangent plane at the point where the surface intersects the measurement line.

In the vicinity of the measurement line the flamelet curves in each illumination plane can be expressed in terms of the principle curvatures of the flamelet surface. Let one laser illumination plane cross the surface tangent plane along a line rotated counterclockwise by an angle θ_p from the x_t axis; the intersection line of the second plane is displaced from the first by 90°. Each illumination plane is inclined at an acute angle to the tangent plane; φ_A for the first plane and φ_B for the second. The specification of the angles θ_p and φ for the two planes defines their orientation with respect to the tangent plane and with respect to x_t and y_t.

The flamelet curves in each illumination plane can be given by sets of points $\{x_p, y_p\}$, where the related axes, x_p and y_p, form a right handed coordinate system in the illumination plane with the x_p axis along the line of intersection between the illumination and tangent planes. It should be noted that φ can be determined from the dot product of $\underline{N}$ and the normal vector defining the orientation in space of the laser illumination sheet.

To relate the measured flamelet curve points $\{x_p, y_p\}$ and the curvatures, one first projects these points onto the tangent plane. In polar coordinates in the tangent plane the projection relationship is given by the following transformation:

$$r = \sqrt{x_p^2 + y_p^2 \cos^2\varphi}$$

$$\theta_t = a\cos\left(x_p \Big/ \sqrt{x_p^2 + y_p^2 \cos^2\varphi} \right) - \theta_p, \qquad (2)$$

where θ_t is the polar angle of the projected point relative to x_t and the inverse cosine term is θ_m, the clockwise angle from the line of intersection between the illumination and the tangent planes to the projected point. Substitution of these points into Eq. (1) gives h_s where the surface intersects the illumination plane.

The altitude of the illumination plane above the tangent plane at points on the flamelet curve is given by

$$h_p = y_p \sin\varphi . \qquad (3)$$

Along the flamelet curve $h_s = h_p$, and by combining equations 1, 2 and 3 one can obtain a relationship between c_x, c_y, θ_p and $\{x_p, y_p\}$.

$$\alpha x_p^2 + \beta x_p y_p - y_p + \gamma y_p^2 = 0, \qquad (4)$$

where $\alpha = (b^2 c_x + c^2 c_y)/d; \beta = 2bc(c_x - c_y)/a;$ and $\gamma = d(c^2 c_x + b^2 c_y)/a^2$.

The coefficients are $a = tan\varphi$, $b = cos\theta_p$, $c = sin\theta_p$ and $d = sin\varphi$. Here θ_p and φ refer to the A or B illumination plane as appropriate.

CPLT images can be processed to give flamelet intersection curves in the two illumination planes as sets of x_p, y_p, points, $\{x_p, y_p\}$. Then to determine c_x, c_y and θ_p, from these points first α, β and γ are found from Eq. (7) by minimizing the sum over $\{x_p, y_p\}$ of the squares of the left hand side. Then the values of α, β and γ given above are used to find the unknown curvatures and angle θ_p.

To test this procedure for finding curvatures a series of numerical experiments were performed. With the relationships presented above, synthetic or phantom flamelet intersection curve data were generated for arbitrary curvature values and arbitrary values of the angles θ_p, φ_a and φ_b defining the two orthogonal laser illumination planes. These synthetic data were analyzed for curvatures and θ_p.

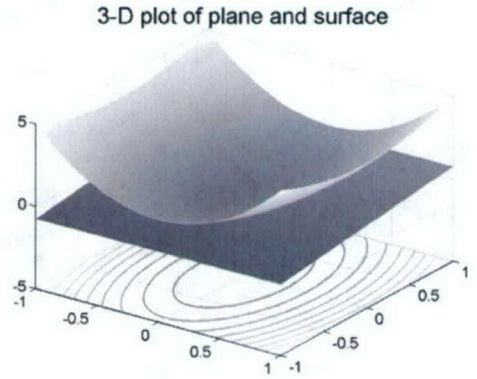

Figure 6a. 3-D plot of "flamelet surface" and illumination plane used to obtain phantom flamelet curve data shown in Figure 6b.

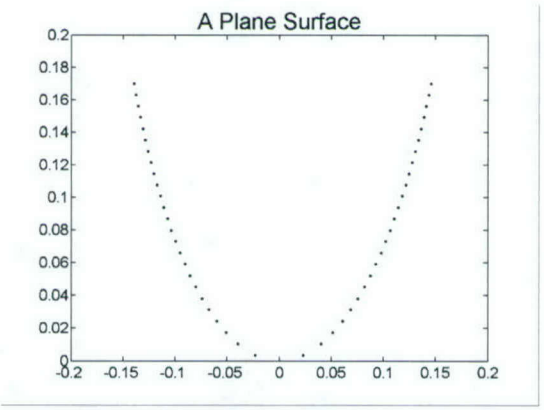

Figure 6b. Phantom flamelet curve data obtained from intersection of surface and plane shown in Figure 6a.

Table 2. Sample Curvature Determination Results

Run	Phi(deg)		Theta (deg)			cx			cy		
#	Plane A	Plane B	actual	Plane A	Plane B	actual	Plane A	Plane B	actual	Plane A	Plane B
1	45.00	45.00	45.00	85.20	85.20	1.00	1.00	1.00	1.00	1.00	1.00
2	45.00	45.00	45.00	45.00	45.00	1.00	1.00	3.00	3.00	3.00	1.00
3	45.00	45.00	45.00	45.00	45.00	1.00	1.00	-3.00	-3.00	-3.00	1.00
4	18.00	59.40	90.00	90.00	0.00	3.00	3.00	3.00	1.00	1.00	1.00
5	18.00	59.40	90.00	90.00	0.00	3.80	3.80	3.80	1.20	1.20	1.20
6	18.00	59.40	0.00	90.00	0.00	3.80	1.20	1.20	1.20	3.80	3.80
7	18.00	59.40	120.00	30.00	30.00	3.80	1.20	3.80	1.20	3.80	1.20
8	36.00	45.00	72.00	72.00	72.00	9.80	9.80	1.50	1.50	1.50	9.80
9	36.00	45.00	178.22	88.22	88.22	3.80	1.20	3.80	1.20	3.80	1.20
10	36.00	45.00	178.82	89.82	89.82	3.80	1.20	3.80	1.20	3.80	1.20

Sample results of these calculations are shown in Figure 5 and presented in Table 2. For the calculations two illumination planes were considered; θ_{pA} for plane A is specified while that for plane B is θ_{pA} plus $\pi/2$. As noted, different values of φ were specific for both planes A and B. From Table 2 it is seen that c_x and c_y can be obtained from curvature data, but θ_p is uncertain by $\pm\pi/2$. θ_p specifies the orientation of the surface in rotation about its normal and is of minimal physical significance. Figure 5 shows the intersections of plane A with the surface of row 9 in the table and the flamelet intersection curve in the A illumination plane, $\{x_p, y_p\}$. The dots on the curves are the individual "data" used for the fits made to find θ_p and the principle curvatures

A preliminary test of the algorithm for finding 3-D curvatures from image data was performed using CPLT images pairs from flame 1 in Table 1. Edge data in the form of third order polynomials of y_p as a function of x_p and in the form of discrete y_p, x_p pairs were used. The results to date have been inconclusive. In the future we will try higher order polynomial fits and review our image processing algorithms for their impact on curvature evaluation.

Swirl Burner: In order to look at a different flame configuration with higher turbulence levels we have built a swirl burner patterned after one developed by Robert Cheng at Lawrence Berkeley Laboratory. The flame in this burner is free standing, Figure 8 and is similar to flames formed behind swirl modules in gas turbine combustors. Figure 7 is a picture (a) and a schematic diagram (b) of the burner, while Figure 8 is a picture of a lean flame stabilized on the burner.

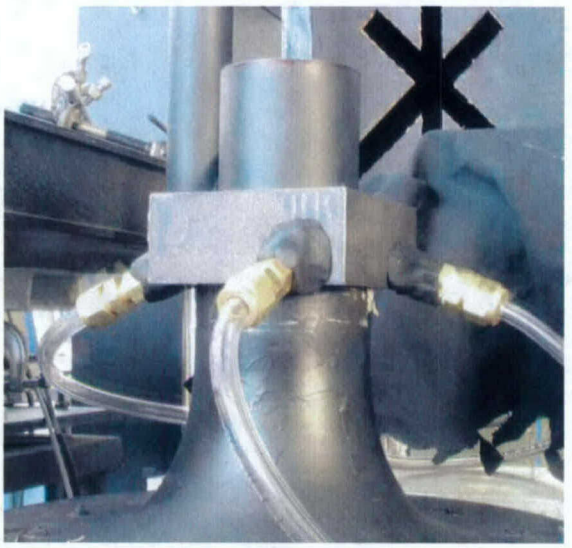

Figure 7a. Picture of new swirl burner showing three of the four swirl air lines.

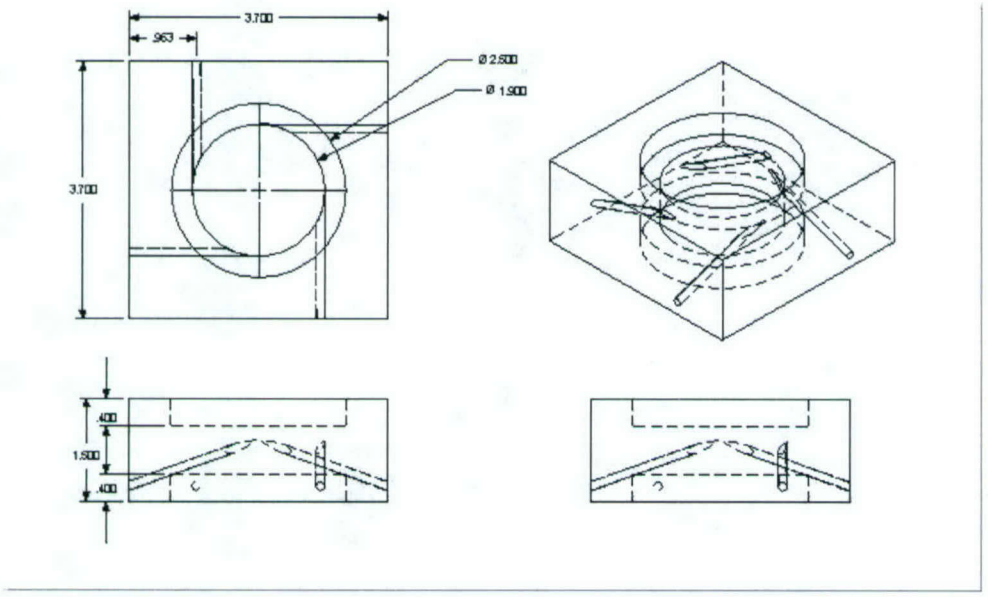

Figure 7b. Schematic diagram of swirl module of the swirl burner. Swirl air is introduced into the burner flow through four jets as shown.

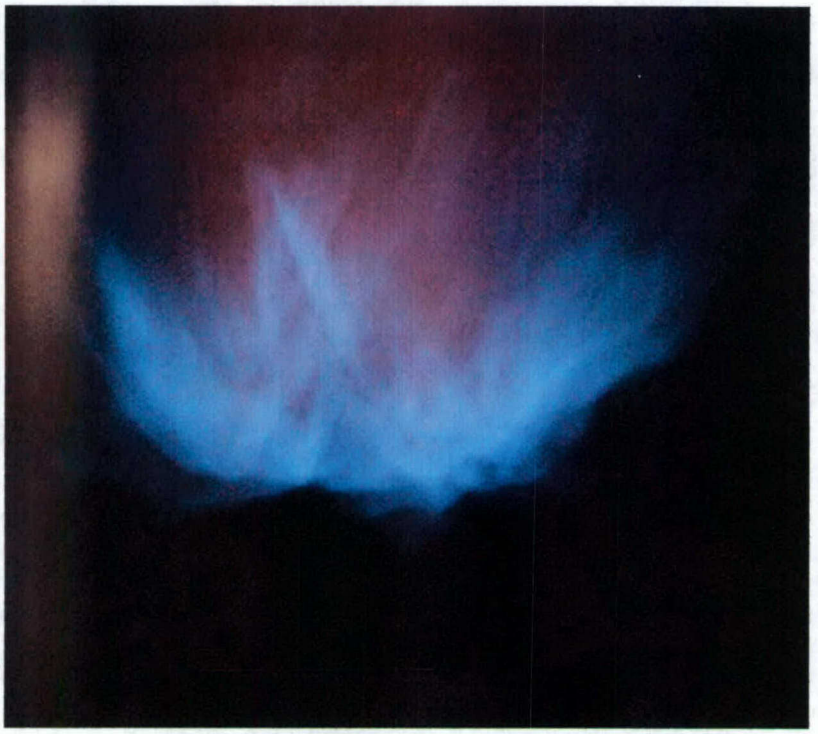

Figure 8. Short time exposure picture of lean ($\phi = 0.7$) methane-air flame.

The stable operating states of the burner at different swirl levels, equivalence ratios and reactants flow rates have been determined and are found to be similar to those reported by Yegian and Cheng [18].

Table 3. Conditions for combined CPT – SPIV Measurements in Swril Flames

• Flame 1:	phi 0.6	U = 2.6 m/s	1200 images
• Flame 2:	phi 0.7	U = 3.2 m/s	1600 images
• Flame 3:	phi 0.7	U = 3.4 m/s	1600 images
• Flame 4:	phi 0.8	U = 2.8 m/s	2000 images
• Flame 5:	phi 0.8	U = 3.0 m/s	2000 images

The data obtained though these measurements are on file but have not been analyzed as of this date.

Summary

We have taken sets of combined CPLT-SPIV data for 11 different methane-air V-flames covering a region of the regime diagram. We have built a new swirl burner and taken a similar data set for five different flame conditions from this burner. From the V-flame image data sets the turbulence properties of the reactant flow, flamelet normal data, displacement speed data and curvature data are being extracted. A method for finding

displacement speed has been demonstrated and one for finding curvature is under development. The swirl burner data will be analyzed in a similar manner. Data of this type will improve our understanding of how turbulence effects premixed flames and will be of value for comparison with the results of direct numerical simulations and of large eddy simulations.

Acknowledgements: Some of this work was initiated during a sabbatical leave of the author at the Combustion Research Facility, Sandia National Laboratories, California. The support of Sandia is gratefully acknowledged. Special thanks are due Drs. Charles Mueller, William Ashurst and Robert Schefer of Sandia for their help

7) References

1. D. C. Bingham, F. C. Gouldin and D. A. Knaus, Crossed-plane laser tomography: Direct measurements of the flamelet surface normal, *Proc. Comb. Inst.* **27**, 77-84 (1998).
2. D. A. Knaus, F. C. Gouldin, P. C Hinze and P. C. Miles, Measurement of instantaneous flamelet surface normals and the burning rate in a SI engine, *SAE Trans.* **108**, paper no. 1999-01-3543 (1999).
3. D. A. Knaus and F. C. Gouldin, Measurements of flamelet orientations in premixed flames with positive and negative Markstein numbers, *Proc. Comb Inst* **28**, 367 (2000).
4. D. A. Knaus, F. C. Gouldin and D. C. Bingham, Assessment of crossed-plane tomography for flamelet surface normal measurements, *Comb Sci. Tech* **174**, 101-134 (2002).
5. S. S. Sattler, F. C. Gouldin and D. A. Knaus, Determination of three-dimensional orientation distributions in turbulent V-flames from two-dimensional image data, *Proc. Comb. Inst.* **29** 1785 (2002).
6. D. A. Knaus, S. S. Sattler and F. C. Gouldin, Crossed-plane Rayleigh imaging for three - dimensional temperature gradients in premixed turbulent flamelets, accepted for publication in *Combustion and Flame*.
7. Sattler, S. S., Gouldin, F. C., and Boertlein, N. T., "Combined crossed-plane imaging and stereo-particle image velocimetry", Joint Meeting of the U.S. Sections of the Combustion Institute, Chicago, IL (2003).
8. P. C. Miles, Conditional velocity statistics and time -resolved flamelet statistics in premixed turbulent V-shaped flames, Ph.D. Thesis, Cornell University, Ithaca, NY 1991.
9. Peters, N., *Turbulent Combustion*, Cambridge University Press, United Kingdom, 2000.
10. Lawson, N. J., and Wu, J., *Meas. Sci. Technol* 8:1455-1464 (1997).
11. Spiegel, M. R. et al, *Probability and Statistics*, 2nd ed., McGraw-Hill, New York, NY, 2000.
12. P. A. Libby, and F. A. Williams, *Comb. Flame* 44: 287-303 (1982).
13. S. H. Sohrab, Z. Y. Ye and C. K. Law, *Proc. Comb. Inst.* 26: 1957 – 1965 (1984).

14. H. N. Najm and P. S. Wyckoff, *Comb. Flame* 110: 92 - 112 (1997).
15. I. R. Gran, T. Echekki, and J. H. Chen, *Proc. Comb. Inst.* 26: 323 – 329 (1998).
16. W. Gellert, H. Küstner, M. Hellwich, et al. (Eds.), *The VNR Concise Encyclopedia of Mathematics*, Van Nostrand Reinhold, New York, (1977) p. 572.
17. S. B. Pope, P. K., Yeung, and S. S. Girimaji, *Phys. Fluids A* 1: 2010-2018 (1989).
18. D. T. Yegian, R. K. Cheng, *Stability characteristics and emission levels of a laboratory hot water heater utilizing a weak-swirl burner*; American Flame Research Council Fall International Symposium, Monterey, CA (US), 15-18 Oct 1995